Design and Performance Analysis of Three-Phase Solar PV Integrated UPQC

Sachin Devassy, *Member, IEEE* and Bhim Singh, *Fellow, IEEE*

Abstract—This paper deals with the design and performance analysis of a three-phase single stage solar photovoltaic integrated unified power quality conditioner (PV-UPQC). The PV-UPQC consists of a shunt and series connected voltage compensators connected back to back with common DC-link.The shunt compensator performs the dual function of extracting power from PV array apart from compensating for load current harmonics. An improved synchronous reference frame control based on moving average filter is used for extraction of load active current component for improved performance of the PV-UPQC. The series compensator compensates for the grid side power quality problems such as grid voltage sags/swells. The compensator injects voltage in-phase/out of phase with point of common coupling (PCC) voltage during sag and swell conditions respectively. The proposed system combines both the benefits of clean energy generation along with improving power quality. The steady state and dynamic performance of the system are evaluated by simulating in Matlab-Simulink under a nonlinear load. The system performance is then verified using a scaled down laboratory prototype under a number of disturbances such as load unbalancing, PCC voltage sags/swells and irradiation variation.

Index Terms—Power Quality, shunt compensator, series compensator, UPQC, Solar PV, MPPT.

I. Introduction

With the advancement in semiconductor technology, there is an increased penetration of power electronic loads. These loads such as computer power supplies, adjustable speed drives, swtiched mode power supplies etc. have very good efficiency, however, they draw nonlinear currents. These nonlinear currents cause voltage distortion at point of common coupling particularly in distribution systems. There is also increasing emphasis on clean energy generation through installation of rooftop PV systems in small apartments as well as in commercial buildings [1], [2]. However, due to the intermittent nature of the PV energy sources, an increased penetration of such systems, particularly in weak distribution systems leads to voltage quality problems like voltage sags and swells, which eventually instability in the grid [3]–[7]. These voltage quality problems also lead to frequent false tripping of power electronic systems, malfunctioning and false triggering of electronic systems and increased heating of capacitor banks etc [8]–[10]. Power quality issues at both load side and grid side are major problems faced by modern distribution systems.

Due to the demand for clean energy as well as stringent power quality requirement of sophisticated electronic loads, there is need for multifunctional systems which can integrate clean energy generation along with power quality improvement. A three phase multi-functional solar energy conversion system, which compensates for load side power quality issues

has been proposed in [11], [12]. A single phase solar pv inverter along with active power filtering capability has been proposed in [13], [14]. Major research work has been done in integrating clean energy generation along with shunt active filtering. Though shunt active filtering has capability for both load voltage regulation, it comes at the cause of injecting reactive power. Thus shunt active filtering cannot regulate PCC voltage as well as maintain grid current unity power factor at same time. Recently, due to the stringent voltage quality requirements for sophsiticated electronics loads, the use of series active filters has been proposed for use in small apartments and commercial buildings [15], [16]. A solar photovoltaic system integrated along with dynamic voltage restorer has been proposed in [17]. Compared to shunt and series active power filters, a unified power quality conditioner (UPQC), which has both series and shunt compensators can perform both load voltage regulation and maintain grid current sinusoidal at unity power factor at same time. Integrating PV array along with UPQC, gives the dual benefits of clean energy generation along with universal active. The integration of PV array with UPQC has been reported in [18]–[20]. Compared to conventional grid connected inverters, the solar PV integrated UPQC has numerous benefits such as improving power quality of the grid, protecting critical loads from grid side disturbances apart from increasing the fault ride through capability of converter during transients. With the increased emphasis on distributed generation and microgrids, there is a renewed interest in UPQC systems [21], [22].

Reference signal generation is a major task in control of PV-UPQC. Reference signal generation techniques can be broadly divided into time-domain and frequency domain techniques [8]. Time domain techniques are commonly used because of lower computational requirements in real-time implementation. The commonly used techniques include instantaneous reactive power theory (p-q theory), synchronous reference frame theory (d-q theory) and instantaneous symmetrical component theory [23]. The main issue in use of synchronous reference frame theory based method is that during load unbalanced condition, double harmonic component is present in the d-axis current. Due to this, low pass filters with very low cut off frequency is used to filter out double harmonic component. This results in poor dynamic performance [24]. In this work, a moving average filter (MAF) is used to filter the d-axis current to obtain fundamental load active current. This gives optimal attenuation and without reducing the bandwidth of the controller [25]. Recently, MAF has been applied in improving performance of DC-link controllers as well as for grid synchronization using phase locked loop (PLL). [26],

[27].

In this paper, the design and performance analysis of a three-phase PV-UPQC are presented. An MAF based d-q theory based control is used to improve the dynamic performance during load active current extraction. The main advantages of the proposed system are as follows,

- Integration of clean energy generation and power quality improvement.
- Simultaneous voltage and current quality improvement.
- Improved load current compensation due to use of MAF in d-q control of PV-UPQC.
- Stable under various dynamic conditions of voltage sags/swells, load unbalance and irradiation variation.

The performance of the proposed system is analyzed extensively under both dynamic and steady state conditions using Matlab-Simulink software. The performance is then experimentally verified using a scaled down laboratory prototype under various conditions experienced in the distribution system such as voltage sags/swells, load unbalance and irradiation variation.

II. SYSTEM CONFIGURATION AND DESIGN

The structure of the PV-UPQC is shown in Fig.1. The PV-UPQC is designed for a three-phase system. The PV-UPQC consists of shunt and series compensator connected with a common DC-bus. The shunt compensator is connected at the load side. The solar PV array is directly integrated to the DC-link of UPQC through a reverse blocking diode. The series compensator operates in voltage control mode and compensates for the grid voltage sags/swells. The shunt and series compensators are integrated to the grid through interfacing inductors. A series injection transformer is used to inject voltage generated by the series compensator into the grid. Ripple filters are used to filter harmonics generated due to switching action of converters. The load used is a nonlinear load consisting of a bridge rectifier with a voltage-fed load.
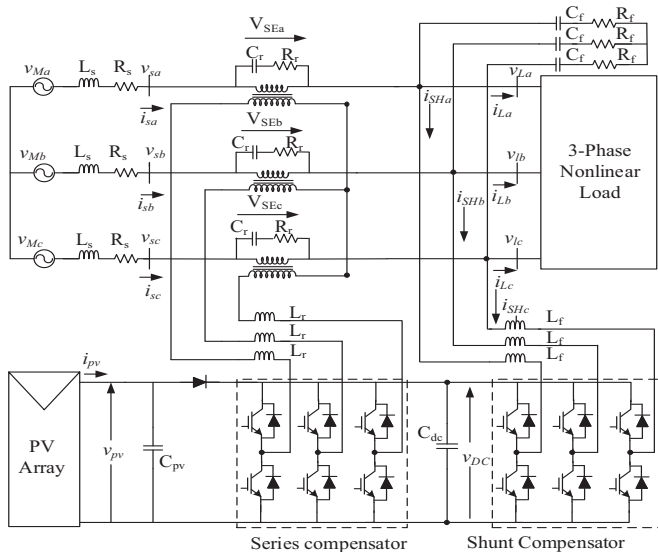

Fig. 1. System Configuration PV-UPQC

A. Design of PV-UPQC

The design procedure for PV-UPQC begins with the proper sizing of PV array, DC-link capacitor, DC-Link voltage level etc. The shunt compensator is sized such that it handles the peak power output from PV array apart from compensating for the load current reactive power and current harmonics. As the PV array is directly integrated to the DC-link of UPQC, the PV array is sized such that the MPP voltage is same as desired DC-link voltage. The rating is such that, under nominal conditions, the PV array supplies the load active power and also feeds power into the grid. The detailed PV array specifications are given in Appendix A. The other designed components are the interfacing inductors of series and shunt compensators and series injection transformer of the series compensator. The design of PV-UPQC is elaborated as follows.

1) Voltage Magnitude of DC-Link: The magnitude of DC-link voltage V_{dc} depends on the depth of modulation used and per-phase voltage of the system. The DC-link voltage magnitude should more than double the peak of per-phase voltage of the three phase system [8] and is given as,

$$V_{dc} = \frac{2\sqrt{2}V_{LL}}{\sqrt{3}m} \qquad (1)$$

where depth of modulation (m) is taken as 1 and V_{LL} is the grid line voltage. For a line voltage of 415 V, the required minimum value DC-bus voltage is 677.7 V. The DC-bus voltage is set at 700 V(approx), which is same as the MPPT operating voltage of PV array at STC conditions.

2) DC-Bus Capacitor Rating: The DC-link capacitor is sized based upon power requirement as well as DC-bus voltage level. The energy balance equation for the DC-bus capacitor is given as follows [8],

$$\begin{aligned}
C_{dc} &= \frac{3kaV_{ph}I_{sh}t}{0.5 \times (V_{dc}^2 - V_{dc1}^2)} \\
&= \frac{3 \times 0.1 \times 1.5 \times 239.6 \times 34.5 \times 0.03}{0.5 \times (700^2 - 677.79^2)} \\
&= 9.3mF
\end{aligned} \qquad (2)$$

where V_{dc} is the average DC-bus voltage, V_{dc1} is the lowest required value of DC-bus voltage, a is the overloading factor, V_{ph} is per-phase voltage, t is the minimum time required for attaining steady value after a disturbance, I_{sh} is per-phase current of shunt compensator, k factor considers variation in energy during dynamics.

The minimum required DC-link voltage is V_{dc1} = 677.69 V as obtained from (2), V_{dc} = 700 V, V_{ph}= 239.60 V,I_{sh}=57.5 A, t= 30 ms, a = 1.2, and for dynamic energy change = 10%, k= 0.1, the value of C_{dc} is obtained as 9.3 mF.

3) Interfacing Inductor for Shunt Compensator: The interfacing inductor rating of the shunt compensator depends upon the ripple current, the switching frequency and DC-link voltage. The expression for the interfacing inductor is as,

$$L_f = \frac{\sqrt{3}mV_{dc}}{12af_{sh}I_{cr,pp}} = \frac{\sqrt{3} \times 1 \times 700}{12 \times 1.2 \times 10000 \times 6.9}$$
$$= 800\mu H \approx 1mH \qquad (3)$$

where m is depth of modulation, a is pu value of maximum overload, f_{sh} is the switching frequency , $I_{cr,pp}$ is the inductor ripple current which is taken as 20% of rms phase current of shunt compensator. Here, m=1, a=1.2, f_{sh}=10kHz, V_{dc}=700V, one gets 800 μH as value. The value chosen is approximated to 1mH.

4) Series Injection Transformer: The PV-UPQC is designed to compensate for a sag/swell of 0.3 pu i.e 71.88 V. Hence, the required voltage to be injection is only 71.88 V which results in low modulation index for the series compensator when the DC-link voltage is 700V. In order to operate the series compensator with minimum harmonics, one keeps modulation index of the series compensator near to unity. Hence a series transformer is used with a turns ratio,

$$K_{SE} = \frac{V_{VSC}}{V_{SE}} = 3.33 \approx 3 \qquad (4)$$

The value obtained for K_{SE} is 3.33. The value selected is 3. The rating of series injection transformer is given as,

$$S_{SE} = 3V_{SE}I_{SE_{sag}} = 3 \times 72 \times 46 = 10kVA \qquad (5)$$

The current through series VSC is same as grid current. The supply current under sag condition of 0.3 pu is 46 A and hence the VA rating of injection transformer achieved is 10 kVA.

5) Interfacing Inductor of Series Compensator: The rating of interfacing inductor of the series compensator depends on ripple current at swell condition, switching frequency and DC-link voltage. Its value is expressed as,

$$L_r = \frac{\sqrt{3} \times mV_{dc}K_{SE}}{12af_{se}I_r} = \frac{\sqrt{3} \times 1 \times 700 \times 3}{12 \times 1.2 \times 10000 \times 7.1}$$
$$= 3.6mH \qquad (6)$$

where m is the depth of modulation, a is the pu value of maximum overload, f_{se} is the switching frequency, I_r is the inductor current ripple, which is taken to be 20% of grid current. Here, m=1, a=1.5, f_{se}=10 kHz, V_{dc}=700 V and 20% ripple current, one gets 3.6 mH as selected value.

III. CONTROL OF PV-UPQC

The main subsystems of PV-UPQC are the shunt compensator and the series compensator. The shunt compensator compensates for the load power quality problems such as load current harmonics and load reactive power. In case of PV-UPQC, the shunt compensator performs the additional function of supplying power from the solar PV array. The shunt compensator extracts power from the PV-array by using a maximum power point tracking (MPPT) algorithm. The series compensator protects the load from the grid side power quality problems such as voltage sags/swells by injecting appropriate voltage in phase with the grid voltage.

A. Control of Shunt Compensator

The shunt compensator extracts the maximum power from the solar PV-array by operating it at its maximum power point. The maximum power point tracking (MPPT) algorithm generates the reference voltage for the DC-link of PV-UPQC.

Some of the commonly used MPPT algorithms [28] are Perturb and Observe (P& O) algorithm, incremental conductance algorithm (INC). In this work, (P& O) algorithm is used for implementing MPPT. The DC-link voltage is maintained at the generated reference by using a PI-controller.

To perform the load current compensation, the shunt compensator extracts the active fundamental component of the load current. For this work, the shunt compensator is controlled by extracting fundamental active component of load current using SRF technique. The control structure of shunt compensator is shown in Fig. 2. The load currents are converted to d-q-0 domain using the phase and frequency information obtained from PLL. The PLL input is the PCC voltage. The d-component of the load current (I_{Ld}) is filtered to extract DC component (I_{Ldf}) which represents the fundamental component in abc frame of reference. To extract DC component without deteriorating the dynamic performance, a moving average filter (MAF) is used to extract the DC component. The transfer function of moving average filter is given as,

$$MAF(s) = \frac{1 - e^{-T_w s}}{T_w s} \qquad (7)$$

where T_w is the window length of the moving average filter. As the lowest harmonic present in the d-axis current is double harmonic component, T_w is kept at half of fundamental time period. The MAF has unity DC gain and zero gain integer multiples of window length.

The equivalent current component due to PV array is given as,

$$I_{pvg} = \frac{2}{3}\frac{P_{pv}}{V_s} \qquad (8)$$

where P_{pv} is the PV array power and V_s is the magnitude of the PCC voltage. The reference grid current in d-axis is given as

$$I_{sd}^* = I_{Ldf} + I_{loss} - I_{pvg} \qquad (9)$$

I_{sd}^* is converted to abc domain reference grid currents. The reference grid currents are compared with the sensed grid currents in a hysteresis current controller to generate the gating pulses for the shunt converter.
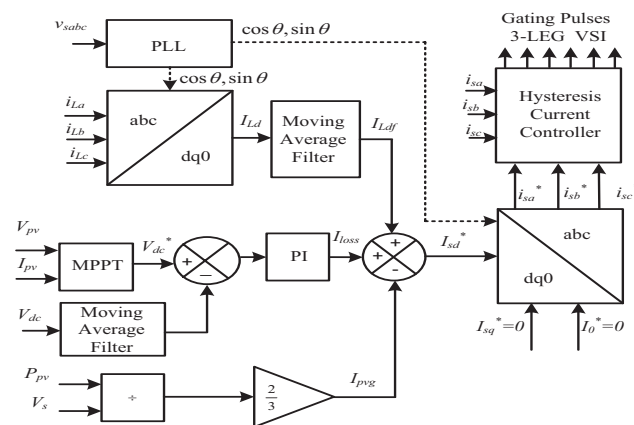

Fig. 2. Control Structure of Shunt Compensator

B. Control of Series Compensator

The control strategy for the series compensator are pre-sag compensation, in-phase compensation and energy optimal compensation. A detailed description of various compensation strategies used for control of series compensator is reported in [29], [30] In this work, the series compensator injects voltage in same phase as that of grid voltage, which results in minimum injection voltage by the series compensator. The control structure of the series compensator is shown in Fig.3. The fundamental component of PCC voltage is extracted using a PLL which is used for generating the reference axis in d-q-0 domain. The reference load voltage is generated using the phase and frequency information of PCC voltage obtained using PLL. The PCC voltages and load voltages are converted into d-q-0 domain. As the reference load voltage is to be in phase with the PCC voltage, the peak load reference voltage is the d-axis component value of load reference voltage. The q-axis component is kept at zero. The difference between the load reference voltage and PCC voltage gives the reference voltage for the series compensator. The difference between load voltage and PCC voltage gives the actual series compensator voltages. The difference between reference and actual series compensator voltages is passed to PI controllers to generate appropriate reference signals. These signals are converted to abc domain and passed through pulse width modulation (PWM) voltage controller to generate appropriate gating signals for the series compensator.
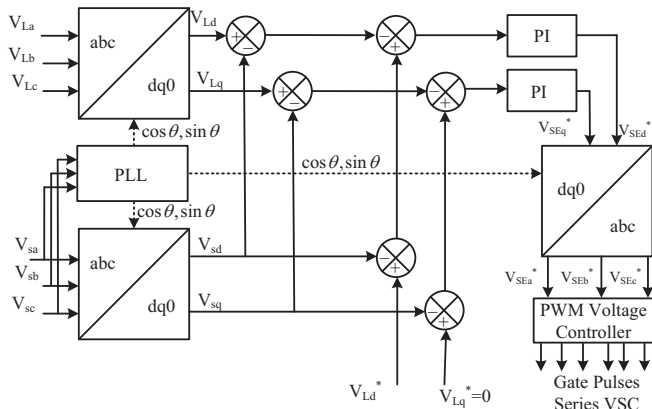

Fig. 3. Control Structure of Series Compensator

IV. SIMULATION STUDIES

The steady state and dynamic performances of PV-UPQC are analyzed by simulating the system in Matlab-Simulink software. The load used is a nonlinear load consisting of three phase diode bridge rectifier with R-L load. The solver step size used for the simulation is 1e-6s. The system is subjected to various dynamic conditions such as sag and swell in PCC voltage and PV irradiation variation. The detailed system parameters are given in Appendix.

A. Performance of PV-UPQC at PCC Voltage Fluctuations

The dynamic performance of PV-UPQC under conditions of PCC voltage sags/swells is shown in Fig.4. The irradiation(G)

is kept at $1000W/m^2$. The various sensed signals are PCC voltages (v_s), load voltages(v_L), series compensator voltages (v_{SE}), DC-link voltage (V_{dc}), solar PV array current (I_{pv}), solar PV array power (P_{pv}), grid currents (i_S), load currents (i_{La}, i_{Lb}, i_{Lc}), shunt compensator currents ($i_{SHa}, i_{SHb}, i_{SHc}$). Between 0.7s and 0.75s, there is voltage sag of 0.3pu and from 0.8s to 0.85s there is voltage swell of 0.3pu. The series compensator compensates for the grid voltage under these conditions by injecting a suitable voltage v_{SE} in opposite phase with the grid voltage disturbance to maintain the load voltage at rated voltage condition.
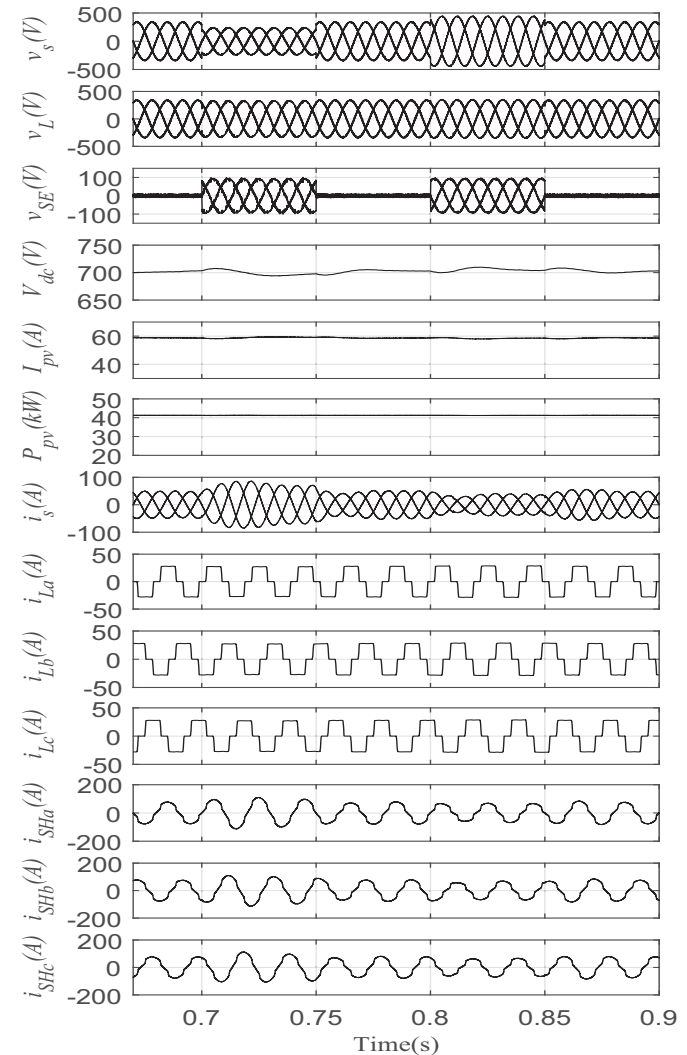

Fig. 4. Performance of PV-UPQC under Voltage Sag and Swell Conditions

B. Performance of PV-UPQC at Load Unbalancing Condition

The dynamic performance of PV-UPQC under load unbalance condition is shown in Fig.5. At t=0.8s, phase 'b' of the load is disconnected. It can be observed that the grid current is sinusoidal and at unity power factor. The current fed into the grid rises leading due to the reduction in the total effective load. The DC-link voltage is also stable and it is maintained near its desired regulated value of 700 V.
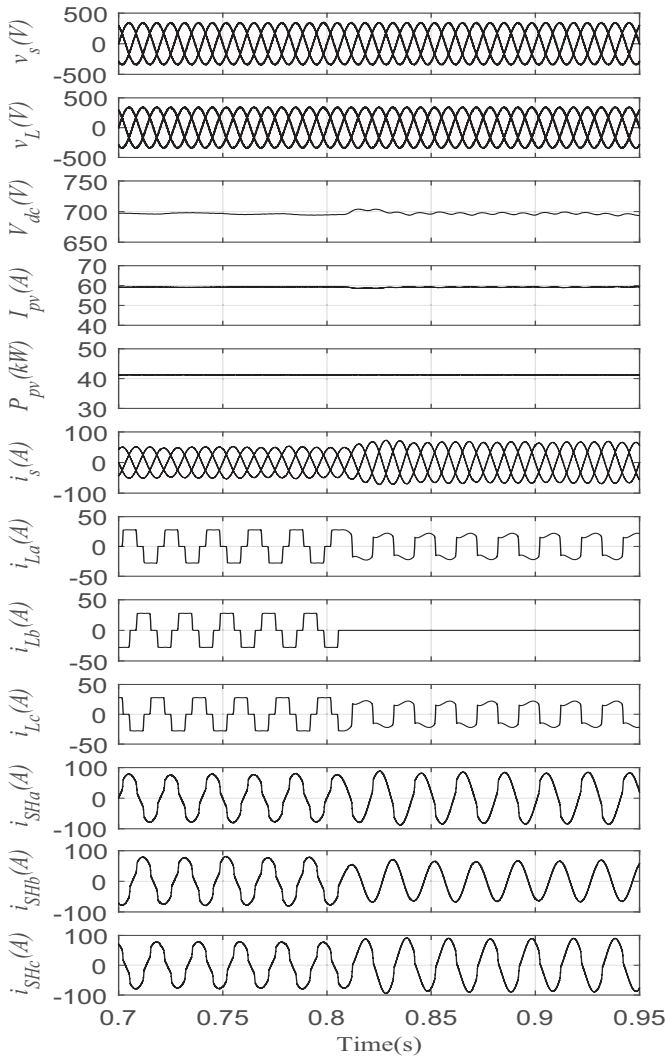
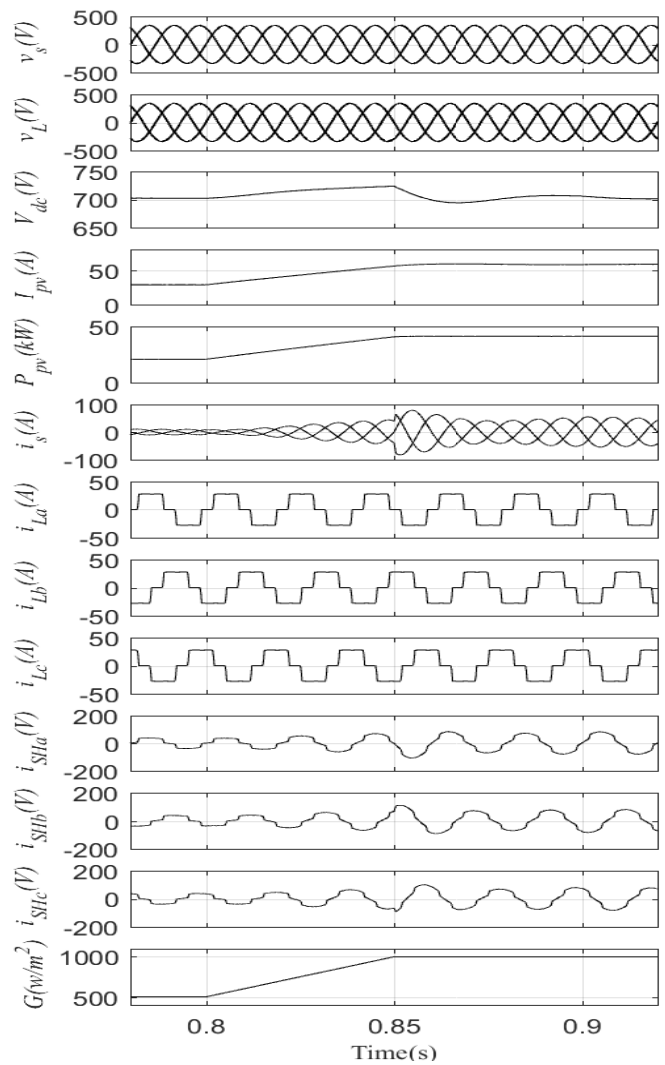Fig. 5. Performance PV-UPQC during Load Unbalance Condition

Fig. 6. Performance PV-UPQC at Varying Irradiation Condition

C. Performance of PV-UPQC under Varying Irradiation

The dynamic performance of PV-UPQC under varying solar irradiation is shown in Fig.6. The solar irradiation is varied from $500 W/m^2$ at 0.8s to $1000 W/m^2$ at 0.85s. It is observed that as irradiation increases, the PV array output increases and hence grid current rises as the PV array is feeding power into the grid. The shunt compensator tracks MPPT along with compensating for the harmonics due to load current.

The harmonic spectra and THD load current and grid current are shown in Fig. 7 and Fig.8. It is observed that the load current THD is 26.31% and the grid current THD is 2.00% thus meeting the requirement of IEEE-519 standard [31].

V. Experimental Results

The PV-UPQC behavior under steady state and dynamic conditions are extensively analyzed on scaled down prototype developed in laboratory. A solar array simulator (AMTEK ETS 600*17DPVF) is used to generate power characteristics similar to a PV array. The shunt and series compensators are realized by using two voltage source converters (SEMIKRON-MD B6CI 750/415-35F) with a common DC-link. The three
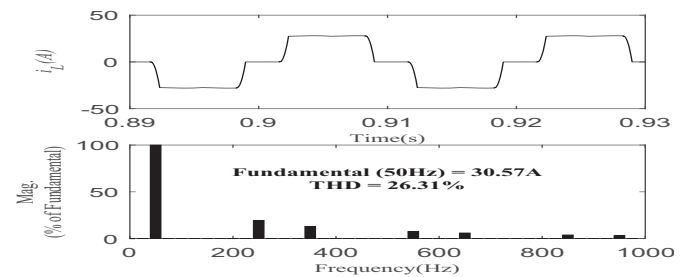

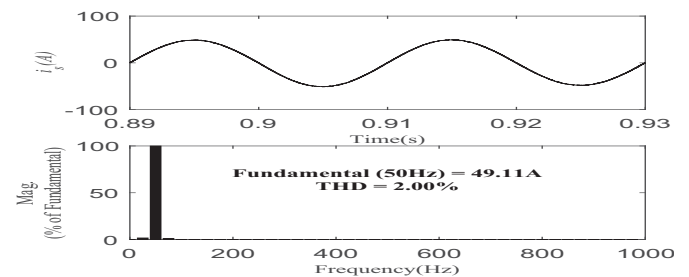Fig. 7. Load Current Harmonic Spectrum and THD

Fig. 8. Grid Current Harmonic Spectrum and THD

phase nonlinear load is realized using a bridge rectifier along with an R-L load. The control is realized using a dSPACE MicrolabBox DSP controller. The performance of the prototype under steady state and dynamic conditions are explained in the following sections. The detailed experimental parameters are given in Appendix.

A. PV-UPQC Operation Under Steady State Condition

The operation of PV-UPQC system under steady state is measured using three phase power analyzer (HIOKI 3310) using 2 wattmeter measurement method. Channels 1 and 2 are used for measuring PCC side voltage, current and power while channels 3 and 4 are used for measuring load side voltage, current and power.

Fig. 9 presents the performance of PV-UPQC system during nominal condition. It can be observed that during nominal condition even though load currents ($I_{La} = Irms3, I_{Lc} = Irms4$) are nonlinear, the grid currents ($I_{sa} = Irms1, I_{sc} = Irms2$) are sinusoidal and at near unity power factor ($\lambda12$). Negative value of PCC power ($P12$) is due to the fact that the power from PV array is more than the load demand ($P34$) and extra power flows into PCC.

Figs. 10 and 11 present the performance of PV-UPQC system during sag and swell conditions. During the voltage sag condition, the PCC voltages ($V_{sab} = Vrms1, V_{scb} = Vrms2$) are at 170V while during swell condition the PCC voltages rise to 270V. It can be observed during both these conditions, the load voltages ($V_{Lab} = Vrms3, V_{Lcb} = Vrms4$) are regulated near the set point of 220 V. The power flows into grid as PV array power exceeds load demand. It can be observed that during all these conditions, the shunt compensator injects active power from PV array and also compensates for load current harmonics and reactive power. It can observed that though the THDs of the load currents ($Ithd3, Ithd4$) are at around 28%, the grid current THDs ($Ithd1, Ithdd2$) are within IEEE-519 limit during nominal conditions.

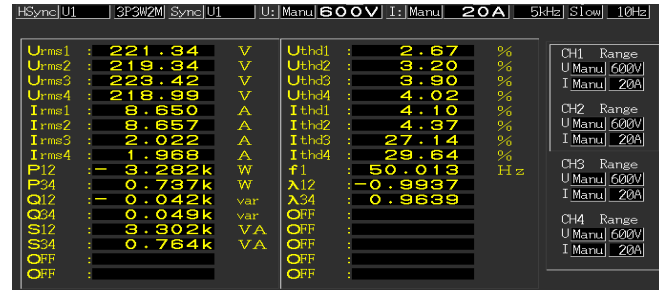### B. PV-UPQC Performance Under Dynamic Condition

Fig. 12 shows the dynamic behavior of PV-UPQC. The response of PV-UPQC is evaluated under various dynamic conditions such as PCC voltage sags/swells, load unbalance condition, and irradiation variation. Figs.12(a) and 12(b) present PV-UPQC response during fluctuations in PCC voltage. The recorded waveforms are PCC line voltage (v_{sab}), load voltage v_{Lab}, series compensator voltage (v_{SEab}), and grid current i_{sa}. Due to the limitations in oscilloscope channels only one phase is shown.

During PCC voltage fluctuations v_{sab} dips to 170 V and rises to 270 V. The series compensator injects voltage in-phase/out-of phase with respect to PCC voltage to maintain v_{Lab} at 220 V. There is rise in i_{sa} during voltage sag condition while there is a decrease in i_{sa} during voltage swell condition, to maintain power balance in the system.

Fig. 12(c) presents PV-UPQC response under unbalanced load condition. The signals presented are V_{dc}, i_{sb}, i_{SHb} and i_{Lb}. The grid current is maintained sinusoidal even though the load is unbalanced. The shunt compensator current is
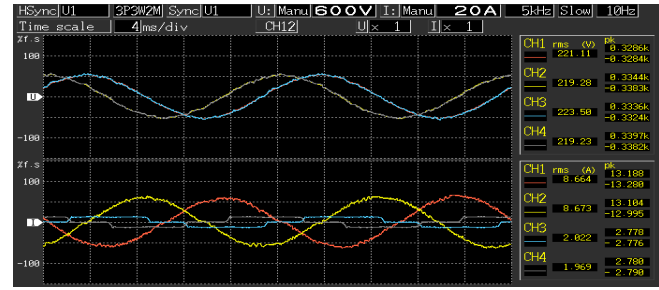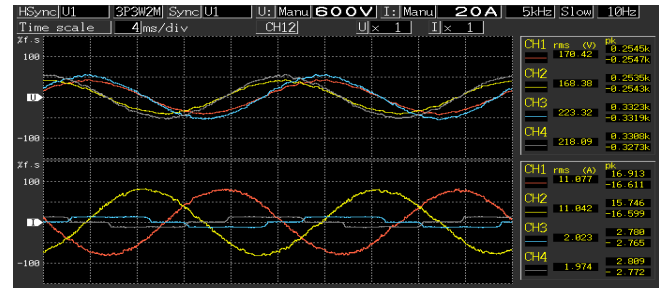

(a) Voltage and Current Waveforms of PCC Side and Load Side During Nominal Condition
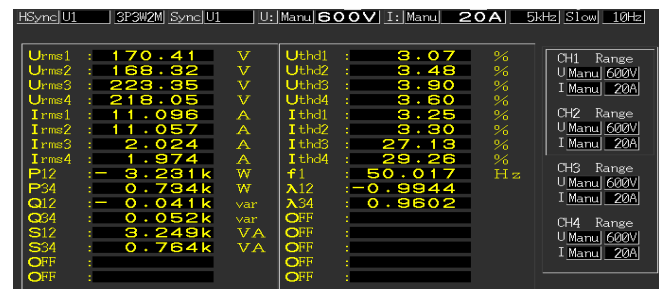

(b) Voltage, Current, Power and THD of PCC Side and Load Side During Nominal Conditions

Fig. 9. PV-UPQC Performance Under Nominal Condition

(a) Voltage and Current Waveforms of PCC Side and Load Side During Sag Condition

(b) Voltage, Current, Power and THD of PCC Side and Load Side During Sag Conditions

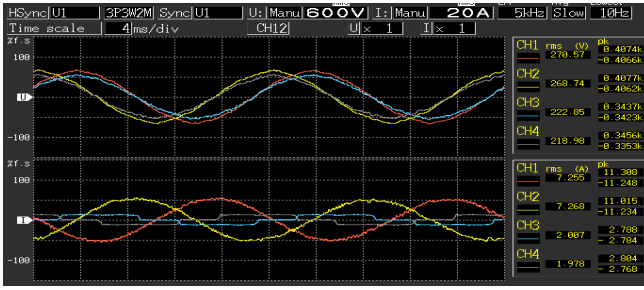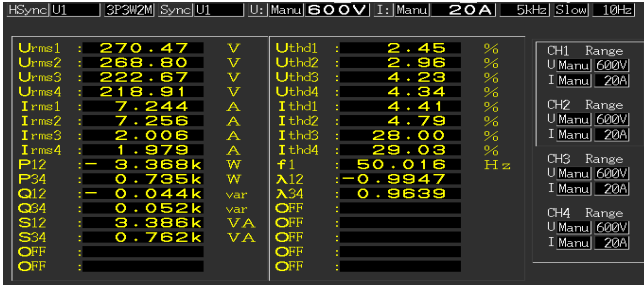Fig. 10. PV-UPQC Performance Under Sag Condition

(a) Voltage and Current Waveforms of PCC Side and Load Side During Sag Condition


(b) Voltage, Current, Power and THD of PCC Side and Load Side During Sag Conditions

Fig. 11. PV-UPQC Performance Under Swell Condition

combination of active current from PV array and load current harmonics. The DC-link voltage V_{dc} is regulated at its desired value. Due to the overall decrease in load power under unbalanced load condition, there is increase in i_{sb} as there is more surplus PV power available to be fed into PCC.
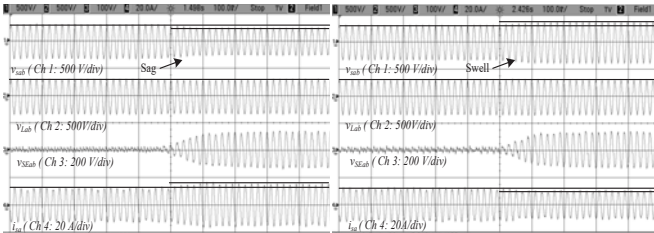
(a) PV-UPQC Behavior Under Sag (b) PV-UPQC Behavior Under Swell
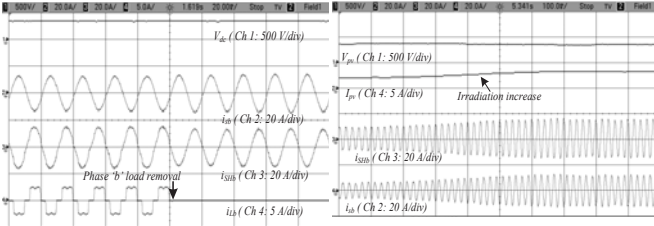
(c) PV-UPQC Behavior under Step Change in Load (d) PV-UPQC Behavior Under Irradiation Change

Fig. 12. Dynamic Performance of PV-UPQC

Fig. 12(d) captures the PV-UPQC response during change in solar irradiation intensity. The waveforms captured are V_{pv}, I_{pv}, i_{SHb} and i_{sb}. The PV irradiation is increased from $500W/m^2$ to $1000W/m^2$. It can be observed that as irradiation increases, the available PV array power increases thus the shunt compensator current and consequently the

current fed into grid increases. Fig. 13 presents tracking efficiency at $1000W/m^2$ and $500W/m^2$. Table. I shows the MPPT efficiency as well as other parameters during the other intermediate irradiation conditions. Under all the irradiation condition,s the system is able to track MPPT with an efficiency more than 99%.
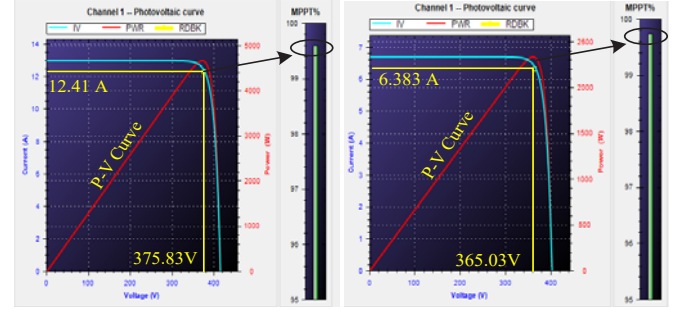
(a) MPPT Tracking Performance at $G = 1000W/m^2$ (b) MPPT Tracking Performance at $G = 500W/m^2$

Fig. 13. MPPT tracking performance of PV-UPQC

The main internal signals involved PV-UPQC control are presented in Fig. 14. Fig. 14(a) captures the internal signals involved in shunt compensator control. The signals captured are load current of phase 'a' i_{La}, load current of phase 'b' i_{Lb}, load current in in d axis in d-q frame I_{Ld} and filtered d-axis load current I_{Ldf}. The internal signals are captured during condition when phase 'b' load is disconnected. It can be observed that load unbalancing results in presence of 100Hz harmonic component in d-axis current. This is then filtered using a moving average filter to extract the DC component which represents the fundamental active component in stationary reference frame.

Fig. 14(b) presents main internal signals involved in series compensator control. The captured signals are d-axis signals of PCC voltage V_{sd}, load voltage v_{Ld}, V_{sed} and q-axis signal of series VSC (V_{seq}). During voltage sag condition, V_{sd} decreases, consequently the V_{SEd} increases thus regulating the V_{Ld} at its desired value. The q-axis component of series voltage is zero showing that the voltage injected by series compensator is in-phase with the PCC voltage.

The performance improvement with the use of MAF in d-q control of PV-UPQC is presented in Fig. 14(c). The signals shown are i_{Lb}, I_{Ld}, filtered d-axis current component using first order low pass filter (I_{Ld_lpf}) and filtered d-axis current component using MAF (I_{Ld_MAF}). It can be observed that even though the cut-off frequency of low pass fiter is 10Hz, there are some ripples present inI_{Ld_lpf}. However, d-axis component filtered using MAF gives very good attenuation and improved dynamic response.

VI. CONCLUSION

The design and dynamic performance of three-phase PV-UPQC have been analyzed under conditions of variable irradiation and grid voltage sags/swells. The performance of the system has been validated through experimentation on scaled down laboratory prototype. It is observed that PV-UPQC mitigates the harmonics caused by nonlinear load and

TABLE I
PV TRACKING EFFICIENCY

SL.No	$G(W/m^2)$	$V_{mpp}(V)$	$I_{mpp}(A)$	$P_{mpp}(W)$	$V_{pv}(V)$	$I_{pv}(A)$	$P_{pv}(W)$	Efficiency(%)
1	1000	371.6	12.6	4672.3	375.8	12.4	4662.6	99.79
2	900	369.9	11.4	4216.1	369.0	11.4	4206.6	99.78
3	800	368.0	10.1	3738.9	370.1	10.1	3738.1	99.97
4	700	365.8	8.9	3255.6	366.3	8.8	3255.6	99.57
5	600	363.3	7.7	2797.4	361.9	7.7	2786.6	99.61
6	500	360.4	6.5	2342.6	365.0	6.4	2336.0	99.74

(a) Internal Signals of Shunt Compensator   (b) Internal Signals of Series Compensator   (c) Performance comparison in Load Active Component Extraction
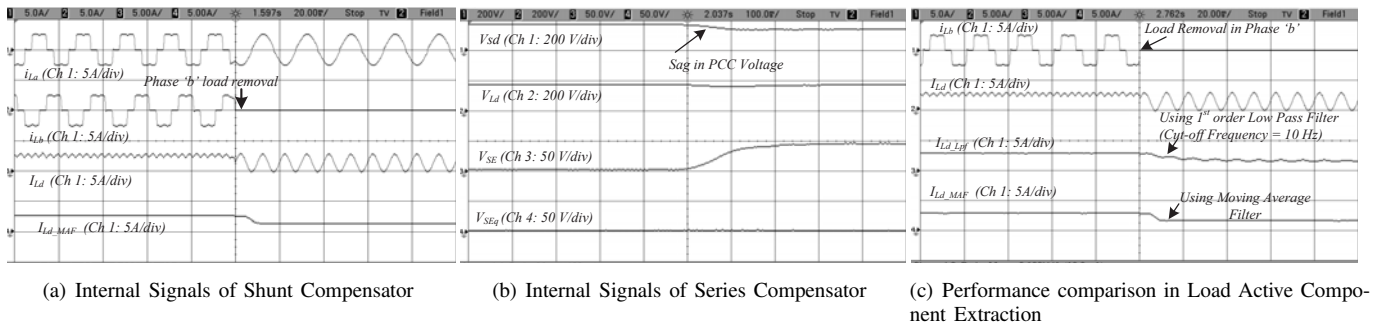
Fig. 14. Salient Internal Signals in PV-UPQC control

maintains the THD of grid current under limits of IEEE-519 standard. The system is found to be stable under variation of irradiation, voltage sags/swell and load unbalance. The performance of d-q control particularly in load unbalanced condition has been improved through the use of moving average filter. It can be seen that PV-UPQC is a good solution for modern distribution system by integrating distributed generation with power quality improvement.

APPENDIX A
SIMULATION PARAMETERS

PCC Line Voltage: 415 V, 50 Hz; Load: Current Fed Bridge Rectifier Load (14.8kW); DC-link Voltage: 700 V; DC-link Capacitor: 9.3 mF; Shunt compensator interfacing inductor: 1 mH; PWM Switching frequency of VSC: 10 kHz; Ripple Filter: 10μF, 10Ω; series compensator interfacing inductor: 3.6 mH; DC-link PI controller gains: $K_p = 1.5$, $K_i = 0.1$; Series VSC PI gains for d and q axis : $K_p = 8$, $K_i = 1200$;

PV array parameters: $V_{oc} = 864$ V, $I_{sc} = 62.65$ A; $V_{mpp} = 701$ V; $I_{mpp} = 58.94$ A; $P_{pv}= 41.35$ kW

APPENDIX B
EXPERIMENTAL PARAMETERS

PCC Line Voltage: 220 V, 50 Hz; Load: Current Fed Bridge Rectifier Load 750 W; DC-link Voltage: 700 V; DC-link Capacitor: 3.3 mF; Shunt compensator interfacing inductor: 4 mH; PWM Switching frequency of VSC: 10 kHz; Ripple Filter: 20μF, 5Ω; series compensator interfacing inductor: 0.5 mH; DC-link PI controller gains: $K_p = 2.5$, $K_i = 1.1$; Series VSC PI gains for d and q axis : $K_p = 5$, $K_i = 800$;

PV array parameters: $V_{oc} = 415$ V, $I_{sc} = 13$ A; $V_{mpp} = 371$ V; $I_{mpp} = 12.57$ A; $P_{pv}= 4.62$ kW

REFERENCES

[1] B. Mountain and P. Szuster, "Solar, solar everywhere: Opportunities and challenges for australia's rooftop pv systems," *IEEE Power and Energy Magazine*, vol. 13, no. 4, pp. 53–60, July 2015.

[2] A. R. Malekpour, A. Pahwa, A. Malekpour, and B. Natarajan, "Hierarchical architecture for integration of rooftop pv in smart distribution systems," *IEEE Transactions on Smart Grid*, vol. PP, no. 99, pp. 1–1, 2017.

[3] Y. Yang, P. Enjeti, F. Blaabjerg, and H. Wang, "Wide-scale adoption of photovoltaic energy: Grid code modifications are explored in the distribution grid," *IEEE Ind. Appl. Mag.*, vol. 21, no. 5, pp. 21–31, Sept 2015.

[4] M. J. E. Alam, K. M. Muttaqi, and D. Sutanto, "An approach for online assessment of rooftop solar pv impacts on low-voltage distribution networks," *IEEE Transactions on Sustainable Energy*, vol. 5, no. 2, pp. 663–672, April 2014.

[5] J. Jayachandran and R. M. Sachithanandam, "Neural network-based control algorithm for DSTATCOM under nonideal source voltage and varying load conditions," *Canadian Journal of Electrical and Computer Engineering*, vol. 38, no. 4, pp. 307–317, Fall 2015.

[6] A. Parchure, S. J. Tyler, M. A. Peskin, K. Rahimi, R. P. Broadwater, and M. Dilek, "Investigating pv generation induced voltage volatility for customers sharing a distribution service transformer," *IEEE Trans. Ind. Appl.*, vol. 53, no. 1, pp. 71–79, Jan 2017.

[7] E. Yao, P. Samadi, V. W. S. Wong, and R. Schober, "Residential demand side management under high penetration of rooftop photovoltaic units," *IEEE Transactions on Smart Grid*, vol. 7, no. 3, pp. 1597–1608, May 2016.

[8] B. Singh, A. Chandra and K. A. Haddad, *Power Quality: Problems and Mitigation Techniques*. London: Wiley, 2015.

[9] M. Bollen and I. Guo, *Signal Processing of Power Quality Disturbances*. Hoboken: Johm Wiley, 2006.

[10] P. Jayaprakash, B. Singh, D. Kothari, A. Chandra, and K. Al-Haddad, "Control of reduced-rating dynamic voltage restorer with a battery energy storage system," *IEEE Trans. Ind. Appl.*, vol. 50, no. 2, pp. 1295–1303, March 2014.

This article has been accepted for publication in a future issue of this journal, but has not been fully edited. Content may change prior to final publication. Citation information: DOI 10.1109/TIA.2017.2754983, IEEE Transactions on Industry Applications

9

[11] B. Singh, C. Jain, and S. Goel, "ILST control algorithm of single-stage dual purpose grid connected solar pv system," *IEEE Trans. Power Electron.*, vol. 29, no. 10, pp. 5347–5357, Oct 2014.

[12] R. K. Agarwal, I. Hussain, and B. Singh, "Three-phase single-stage grid tied solar pv ecs using PLL-less fast CTF control technique," *IET Power Electronics*, vol. 10, no. 2, pp. 178–188, 2017.

[13] Y. Singh, I. Hussain, B. Singh, and S. Mishra, "Single-phase solar grid-interfaced system with active filtering using adaptive linear combiner filter-based control scheme," *IET Generation, Transmission Distribution*, vol. 11, no. 8, pp. 1976–1984, 2017.

[14] T.-F. Wu, H.-S. Nien, C.-L. Shen, and T.-M. Chen, "A single-phase inverter system for pv power injection and active power filtering with nonlinear inductor consideration," *IEEE Trans. Ind. Appl.*, vol. 41, no. 4, pp. 1075–1083, July 2005.

[15] A. Javadi, A. Hamadi, L. Woodward, and K. Al-Haddad, "Experimental investigation on a hybrid series active power compensator to improve power quality of typical households," *IEEE Trans. Ind. Electron.*, vol. 63, no. 8, pp. 4849–4859, Aug 2016.

[16] A. Javadi, L. Woodward, and K. Al-Haddad, "Real-time implementation of a three-phase thseaf based on vsc and p+r controller to improve power quality of weak distribution systems," *IEEE Transactions on Power Electronics*, vol. PP, no. 99, pp. 1–1, 2017.

[17] A. M. Rauf and V. Khadkikar, "Integrated photovoltaic and dynamic voltage restorer system configuration," *IEEE Transactions on Sustainable Energy*, vol. 6, no. 2, pp. 400–410, April 2015.

[18] S. Devassy and B. Singh, "Design and performance analysis of three-phase solar pv integrated upqc," in *2016 IEEE 6th International Conference on Power Systems (ICPS)*, March 2016, pp. 1–6.

[19] K. Palanisamy, D. Kothari, M. K. Mishra, S. Meikandashivam, and I. J. Raglend, "Effective utilization of unified power quality conditioner for interconnecting PV modules with grid using power angle control method," *International Journal of Electrical Power and Energy Systems*, vol. 48, pp. 131 – 138, 2013.

[20] S. Devassy and B. Singh, "Modified p-q theory based control of solar pv integrated upqc-s," *IEEE Trans. Ind. Appl.*, vol. PP, no. 99, pp. 1–1, 2017.

[21] S. K. Khadem, M. Basu, and M. F. Conlon, "Intelligent islanding and seamless reconnection technique for microgrid with upqc," *IEEE Journal of Emerging and Selected Topics in Power Electronics*, vol. 3, no. 2, pp. 483–492, June 2015.

[22] J. M. Guerrero, P. C. Loh, T. L. Lee, and M. Chandorkar, "Advanced control architectures for intelligent microgrids;part ii: Power quality, energy storage, and ac/dc microgrids," *IEEE Transactions on Industrial Electronics*, vol. 60, no. 4, pp. 1263–1270, April 2013.

[23] B. Singh and J. Solanki, "A comparison of control algorithms for dstatcom," *IEEE Transactions on Industrial Electronics*, vol. 56, no. 7, pp. 2738–2745, July 2009.

[24] B. Singh, C. Jain, S. Goel, A. Chandra, and K. Al-Haddad, "A multifunctional grid-tied solar energy conversion system with anf-based control approach," *IEEE Transactions on Industry Applications*, vol. 52, no. 5, pp. 3663–3672, Sept 2016.

[25] S. Golestan, M. Ramezani, J. M. Guerrero, and M. Monfared, "dq-frame cascaded delayed signal cancellation- based pll: Analysis, design, and comparison with moving average filter-based pll," *IEEE Transactions on Power Electronics*, vol. 30, no. 3, pp. 1618–1632, March 2015.

[26] R. Pea-Alzola, D. Campos-Gaona, P. F. Ksiazek, and M. Ordonez, "Dc-link control filtering options for torque ripple reduction in low-power wind turbines," *IEEE Trans. Power Electron.*, vol. 32, no. 6, pp. 4812–4826, June 2017.

[27] S. Golestan, M. Ramezani, J. M. Guerrero, F. D. Freijedo, and M. Monfared, "Moving average filter based phase-locked loops: Performance analysis and design guidelines," *IEEE Trans. Power Electron.*, vol. 29, no. 6, pp. 2750–2763, June 2014.

[28] B. Subudhi and R. Pradhan, "A comparative study on maximum power point tracking techniques for photovoltaic power systems," *IEEE Transactions on Sustainable Energy*, vol. 4, no. 1, pp. 89–98, Jan 2013.

[29] A. Sadigh and K. Smedley, "Review of voltage compensation methods in dynamic voltage restorer DVR," in *IEEE Power and Energy Society General Meeting*, July 2012, pp. 1–8.

[30] A. Rauf and V. Khadkikar, "An enhanced voltage sag compensation scheme for dynamic voltage restorer," *IEEE Trans. Ind. Electron.*, vol. 62, no. 5, pp. 2683–2692, May 2015.

[31] "IEEE recommended practices and requirements for harmonic control in electrical power systems," *IEEE Std 519-1992*, pp. 1–112, April 1993.

Sachin Devassy (S'15, M'17) received B. Tech in Electrical and Electronics Engineering in 2007 from Govt. Engineering College, Thrissur, Kerala, India. He received M. Tech in Power Electronics, Electrical Machines and Drives from IIT Delhi in 2010. He is currently working towards his PhD degree in the Department of Electrical Engineering, IIT Delhi, New Delhi, India. He has been working in Power Electronics Group at CSIR-CEERI since July 2010. His areas of research interest include power electronics, power quality, custom power devices and renewable energy systems.

Bhim Singh (SM'99, F'10) was born in Rahamapur, Bijnor (UP), India, in 1956. He received his B.E. (Electrical) from the University of Roorkee, India, in 1977 and his M.Tech. (Power Apparatus & Systems) and Ph.D. from the Indian Institute of Technology Delhi, India, in 1979 and 1983, respectively. In 1983, he joined the Department of Electrical Engineering, University of Roorkee (Now IIT Roorkee), as a Lecturer. He became a Reader there in 1988. In December 1990, he joined the Department of Electrical Engineering, IIT Delhi, India, as an Assistant Professor, where he has become an Associate Professor in 1994 and a Professor in 1997. He has been ABB Chair Professor from September 2007 to September 2012. Since October 2012, he is CEA Chair Professor. He has been Head of the Department of Electrical Engineering at IIT Delhi from July 2014 to August 2016. Since, August 2016, he is the Dean, Academics at IIT Delhi. He is JC Bose Fellow of DST, Government of India since December 2015. Prof. Singh has guided 65 Ph.D. dissertations, 167 M.E./M.Tech./M.S.(R) theses, and 60 BE/B.Tech. Projects. He has been filed 23 patents. He has executed more than eighty sponsored and consultancy projects. He has co-authored a text book on power quality: Power Quality Problems and Mitigation Techniques published by John Wiley & Sons Ltd. 2015. His areas of interest include solar PV grid interface systems, microgrids, power quality monitoring and mitigation, solar PV water pumping systems, improved power quality AC-DC converters, power electronics, electrical machines, drives, FACTS, and high voltage direct current (HVDC) systems. Prof. Singh is a Fellow of the Indian National Academy of Engineering (FNAE), The Indian National Science Academy (FNA), The National Academy of Science, India (FNASc), The Indian Academy of Sciences, India (FASc), The World Academy of Sciences (FTWAS), Institute of Electrical and Electronics Engineers (FIEEE), the Institute of Engineering and Technology (FIET), Institution of Engineers (India) (FIE), and Institution of Electronics and Telecommunication Engineers (FIETE) and a Life Member of the Indian Society for Technical Education (ISTE), System Society of India (SSI), and National Institution of Quality and Reliability (NIQR). He has received Khosla Research Prize of University of Roorkee in the year 1991. He is recipient of JC Bose and Bimal K Bose awards of The Institution of Electronics and Telecommunication Engineers (IETE) for his contribution in the field of Power Electronics. He is also a recipient of Maharashtra State National Award of Indian Society for Technical Education (ISTE) in recognition of his outstanding research work in the area of Power Quality. He has received PES Delhi Chapter Outstanding Engineer Award for the year 2006. Professor Singh has received Khosla National Research Award of IIT Roorkee in the year 2013. He has also received Shri Om Prakash Bhasin Award-2014 in the field of Engineering including Energy & Aerospace. He has been the General Chair of the 2006 IEEE International Conference on Power Electronics, Drives and Energy Systems (PEDES2006), General Co-Chair of the 2010 IEEE International Conference on Power Electronics, Drives and Energy Systems (PEDES2010), General Co-Chair of the 2015 IEEE International Conference (INDICON2015), General Co-Chair of 2016 IEEE International Conference (ICPS2016) held in New Delhi.